International Journal of Power Electronics and Drive System (IJPEDS)
Vol. 17, No. 1, March 2026, pp. 617~628
ISSN: 2088-8694, DOI: 10.11591/ijpeds.v17.i1.pp617-628

A novel high-gain DC-DC converter with fuzzy logic control for hydrogen fuel cell vehicle applications

Gaddala Anusha[1], A. V. V. Sudhakar[1], Shaik Rafikiran[2], Ram Ragotham Deshmukh[1], C. H. Hussaian Basha[1]
[1]Department of Electrical and Electronics Engineering, S. R. University, Warangal, India
[2]Department of Electrical and Electronic Engineering, Sri Venkateswara College of Engineering, Andhra Pradesh, India

Article Info

Article history:

Received Feb 19, 2025
Revised Nov 21, 2025
Accepted Dec 11, 2025

Keywords:

Electric vehicles
Energy management
Fuzzy logic control
High-gain DC-DC converter
Hydrogen fuel cell

ABSTRACT

Hydrogen fuel cell vehicles (HFCVs) are emerging as a sustainable alternative to conventional internal combustion engines due to their zero-emission characteristics and high energy efficiency. However, the low output voltage of fuel cells poses a significant challenge in meeting the high-voltage requirements of electric traction systems. To address this, this paper proposes a high-gain non-isolated switched-capacitor (SC) DC-DC converter integrated with a fuzzy logic controller (FLC) for efficient power management in hydrogen fuel cell vehicle applications. The proposed converter topology achieves a significant voltage step-up without the use of bulky magnetic components, making it lightweight and compact for automotive integration. A maximum power point tracking (MPPT) controller using fuzzy logic is used to recover optimum energy out of the fuel cell stack during different loads and conditions of the environment. MATLAB/Simulink simulation results validate the high voltage gain, stable operation, and improved dynamic response of the proposed converter under FLC control. The proposed intelligent control strategy enhances fuel cell utilization and ensures effective operation of HFCV powertrains.

Corresponding Author:

C. H. Hussaian Basha
Department of Electrical and Electronics Engineering, S. R. University
Warangal-506371, India
Email: hussaian.basha@sru.edu.in

1. INTRODUCTION

The increasing trend towards clean transportation has raised interest in hydrogen fuel cell vehicles (HFCVs), which are highly efficient and zero-emitting. Nevertheless, proton exchange membrane fuel cells (PEMFCs) have low and variable output voltage (30-60 V) which is not sufficient to power a traction inverter which needs voltages more than 300 V. Thus, DC- DC converter with an intelligent control strategy is required to provide stable power output in HFCV systems Figure 1 shows the Proposed single switch high voltage conversion ratio (SSHVCR) converter with fuzzy logic MPPT for fuel cell applications [1]. Traditional boost converters are inefficient at very high duty cycles and have high component stress, large magnetic components and do not respond well to very dynamic operation; they are not suitable for very small automotive systems. Recently, switched capacitor (SC) converters have also been in the limelight because they can be designed to have high gain with no magnetic elements, so that the converter is both lightweight and compact. However, voltages and converters still face limitations such as output ripple, unbalanced capacitor voltages, and weakened dynamic performance under variable load conditions [2].

To address these challenges, this paper presents a novel non-isolated high-gain switched-capacitor DC–DC converter (SSHVCR) integrated with a fuzzy logic controller (FLC)-based maximum power point tracking (MPPT) technique for fuel-cell vehicle applications. The proposed SSHVCR topology provides a voltage gain exceeding 300 V from a 30–60 V input without bulky magnetics, while maintaining reduced switch stress and uniform current distribution [3]. The FLC-based MPPT further enhances fuel-cell utilization by offering faster convergence, smoother tracking, and improved robustness compared with classical Perturb & Observe (P&O) and incremental conductance (IC) methods. Figure 2 shows the input and output variables in the fuzzy logic MPPT controller. The work contributes by: i) proposing a compact high-gain converter suitable for automotive integration, ii) developing an FLC-based MPPT controller optimized for nonlinear SC converter behavior, and iii) validating the system through MATLAB/Simulink simulations. The results demonstrate high conversion gain, low ripple, fast dynamic response, and enhanced MPPT accuracy, demonstrating the converter's suitability for next-generation hydrogen fuel cell vehicles [4].

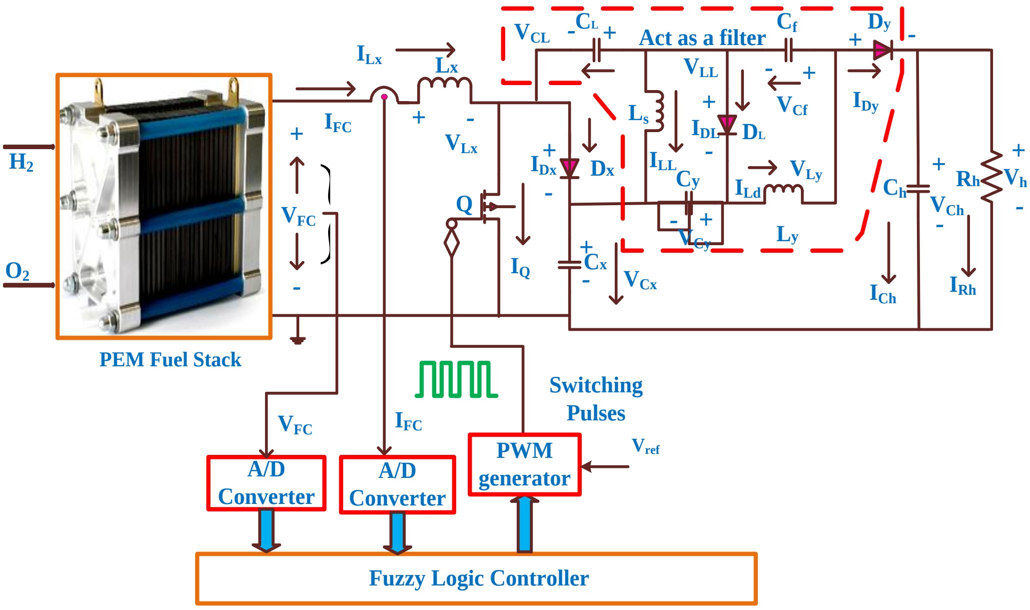

Figure 1. Block diagram of the proposed SSHVCR converter with fuzzy logic MPPT for fuel cell applications [5]

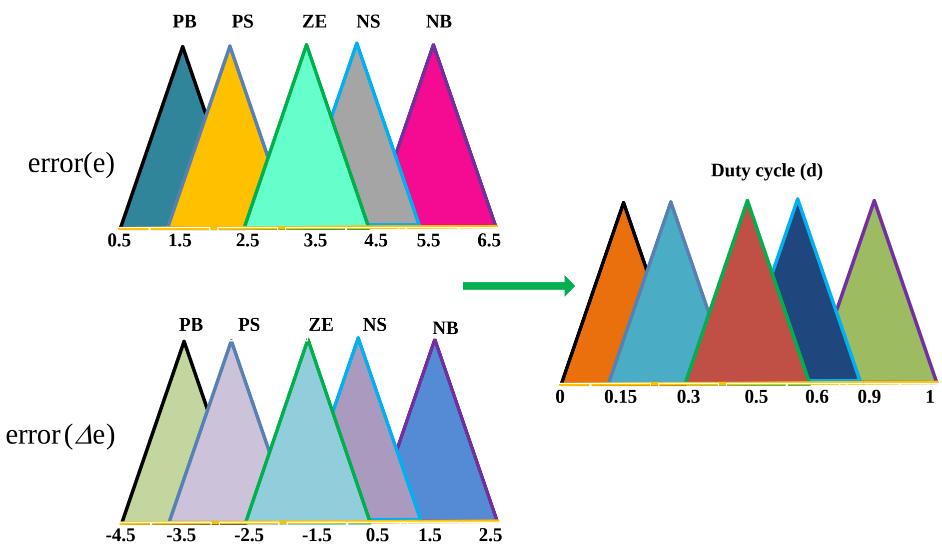

Figure 2. The input and output variables in the fuzzy logic MPPT controller [6]

2. METHOD

2.1. Fuel cell modelling

PEMFCs are widely used in automotive systems due to their low operating temperature, fast start-up, and high-power density. The electrochemical reaction converts hydrogen and oxygen into water while producing electrical energy [7]:

$$H_2 + \frac{1}{2}O_2 \rightarrow H_2O + \text{Energy} \quad (1)$$

The actual cell voltage is expressed as (2).

$$V_{cell} = E_{Nernst} - V_{act} - V_{ohmic} - V_{conc} \quad (2)$$

The (1) describes the electrochemical reaction occurring in a PEM fuel cell, where hydrogen and oxygen combine to produce water and electrical energy. The practical output voltage of the fuel cell is defined in (2), where the ideal Nernst voltage is reduced by activation, ohmic, and concentration losses [8]. The reversible open-circuit voltage is calculated using the Nernst equation given in (3).

$$E_{Nernst} = E^0 + \frac{RT}{2F}\ln\left(\frac{P_{H_2}\cdot\sqrt{P_{O_2}}}{P_{atm}}\right) \quad (3)$$

Activation losses follow the Tafel:

$$V_{act} = \frac{RT}{\alpha nF}\ln\left(\frac{i}{i_0}\right) \quad (4)$$

Ohmic losses, dominated by ionic resistance of the membrane, increase linearly with current:

$$V_{ohmic} = i \cdot R_{ohmic} \quad (5)$$

Concentration losses appear at high current densities as reactants are depleted at electrode surfaces:

$$V_{conc} = -B\ln\left(1 - \frac{i}{i_{lim}}\right) \quad (6)$$

The reversible open-circuit voltage is calculated using the Nernst in (3), which accounts for the effects of operating temperature and reaction partial pressures. The activation overpotential, associated with electrochemical reaction kinetics at the electrodes, is modeled using the Tafel in (4). Ohmic losses arising from ionic and electronic resistances within the membrane and cell components are represented by (5), showing a linear dependence on current. At high current densities, concentration overpotential becomes significant due to mass transport limitations, as expressed in (6) [9].

A typical fuel-cell stack consists of multiple cells connected in series:

$$V_{stack} = N \cdot V_{cell} \quad (7)$$

The output power is:

$$P_{stack} = V_{stack} \cdot I \quad (8)$$

For practical applications, multiple cells are connected in series to form a stack, and the resulting stack voltage is given in (7). Finally, the electrical output power of the fuel-cell stack is determined using (8), which relates the stack voltage and operating current. This model captures the non-linear voltage–current behaviour of PEMFCs and enables accurate simulation under variable load conditions [10]. It also provides the basis for integrating MPPT control to maximize energy extraction. Figure 3 illustrates the Representation of PEMFC operation [11].

2.2. Maximum power point tracking (MPPT) technique

Fuel cell voltage and power vary with load, temperature, and pressure. To ensure maximum extraction of available energy, MPPT is essential. Three common techniques, perturb and observe (P&O), IC, and FLC, are considered [13]. Figure 4 indicates the annual publication trend of MPPT-Related Articles in IEEE and Elsevier Journals.

Figure 4 presents the annual trend of MPPT-related publications from 2012 to 2025. The x-axis denotes the publication year, while the y-axis represents the number of published articles per year. IEEE and Elsevier journal publications are distinguished using green and purple bars, respectively, enabling clear comparative analysis.

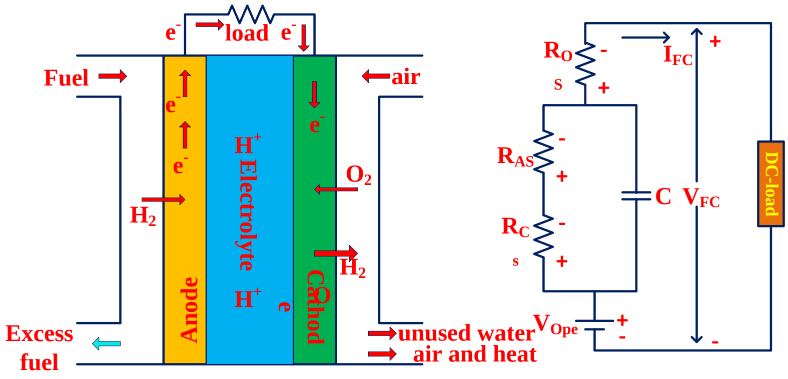

Figure 3. Schematic representation of PEMFC operation [12]

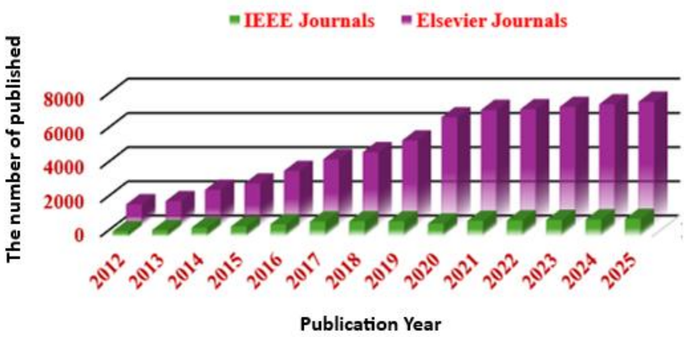

Figure 4. Annual publication trend of MPPT-related articles in IEEE and Elsevier Journals (2012-2025) [14]

2.2.1. P&O algorithm

P&O perturbs the operating voltage and observes the resulting power change:

$$P = V \cdot I \quad (9)$$

If $\Delta P/\Delta V > 0$, the voltage is increased; otherwise, it is decreased. Although simple, this method suffers from oscillations around the MPP and performs poorly under rapid transients.

2.2.2. IC technique

IC improves accuracy by using:

$$\frac{dP}{dV} = 0 \Rightarrow \frac{d(VI)}{dV} = I + V\frac{dI}{dV} = 0 \Rightarrow \frac{dI}{dV} = -\frac{I}{V} \quad (10)$$

If:

$\frac{dI}{dV} > -\frac{I}{V}$: increase V

$\frac{dI}{dV} < -\frac{I}{V}$: decrease V

IC responds faster than P&O but requires more computation and still exhibits moderate ripples [15].

2.2.3. Fuzzy logic controller (FLC)

FLC is well-suited for nonlinear systems like switched-capacitor converters. It uses:

$$\text{Error } E(k) = \frac{dP}{dV} \quad (11)$$

$$\text{Change in Error } \Delta E(k) = E(k) - E(k-1) \quad (12)$$

These two variables are fed into fuzzy rules to generate the duty cycle adjustment. FLC does not require system modelling, handles uncertainty effectively, and provides fast, smooth tracking with minimal oscillations. Figure 5 functional architecture of the fuzzy logic-based MPPT controller.

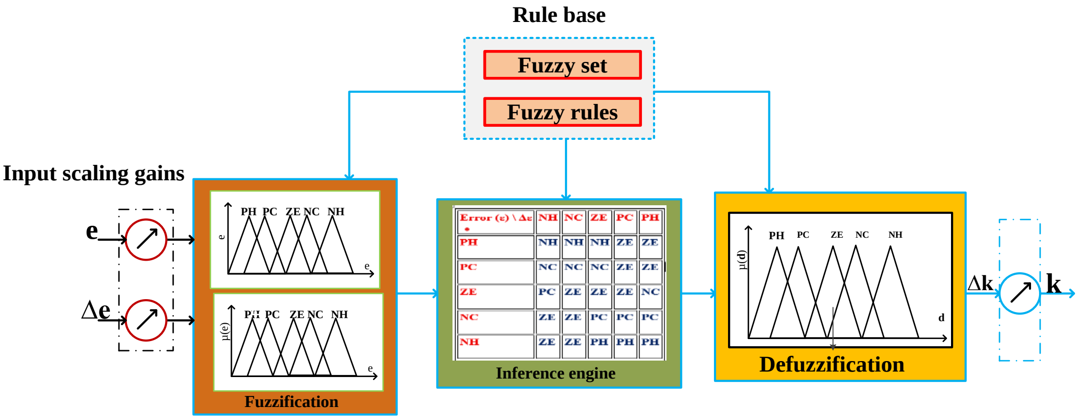

Figure 5. Functional architecture of the fuzzy logic-based MPPT controller [16]

3. MODELLING AND PRACTICAL IMPLEMENTATION OF THE SSHVCR CONVERTER

The proposed single-switch high-voltage conversion ratio (SSHVCR) converter consists of an input inductor L_a, main MOSFET switch S, diodes, and a switched-capacitor network formed by C_x, C_d, C_e, C_q. This structure enables high voltage gain by transferring charges through cascaded capacitor groups across different switching intervals. The converter operates in three modes depending on the state of the MOSFET. Figures 6 (a)–(c) illustrate the operating stages [17]. Figure 7 shows the operating modes of the SSHVCR DC-DC converter.

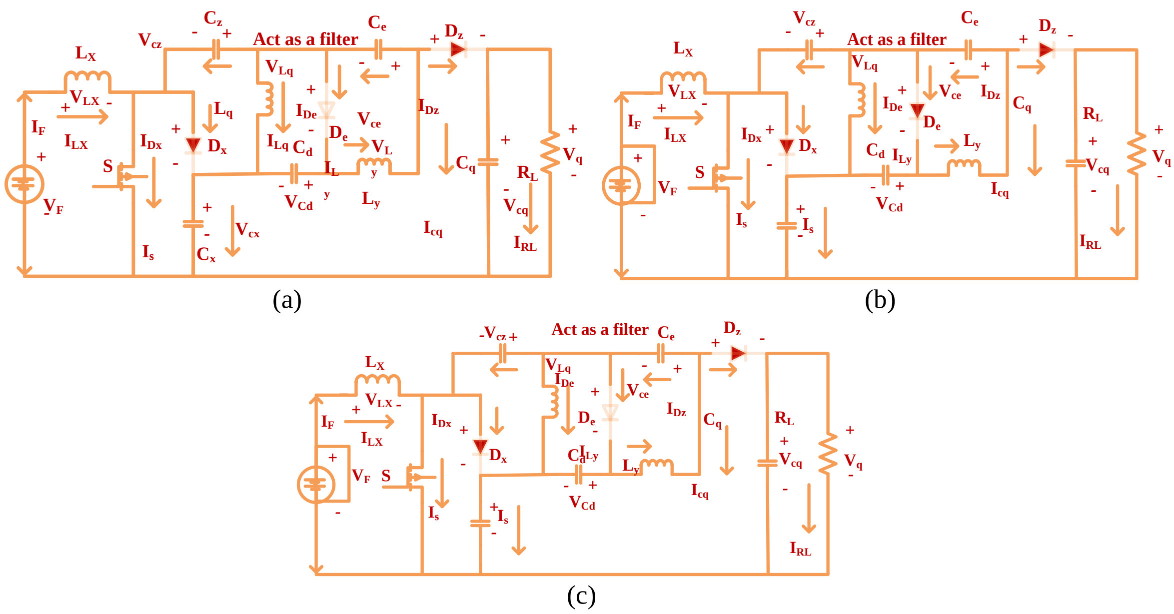

Figure 6. Operating modes of the proposed SSHVCR DC–DC converter: (a) switch ON, (b) switch OFF (capacitor charging), and (c) energy transfer to the load [18]

3.1. Working on a converter at the mode-I stage

When the MOSFET is turned ON, the input inductor $L_a$stores energy while capacitors on the secondary side maintain their previous charge states. Diodes become reverse-biased, preventing current flow toward the output. The inductor voltage and current during this stage are obtained using [19]:

$$\begin{cases} I_{Ce-cing} = I_{Cz-ding} = I_{Le} + I_{Ld} \\ I_{Cd-ding} = I_{Cf-cing} = I_{Ld} \\ I_{Cg-ding} = I_{Rg} \end{cases} \quad (13)$$

$$\begin{cases} V_{Lz} = V_F \\ V_{Le} = V_{Cz} - V_{Ce} \\ V_{Ld} = V_{Cz} + V_{Ce} - V_{Cd} - V_{Cq} \end{cases} \quad (14)$$

During this interval, the inductor current increases linearly, and no power is delivered to the load.

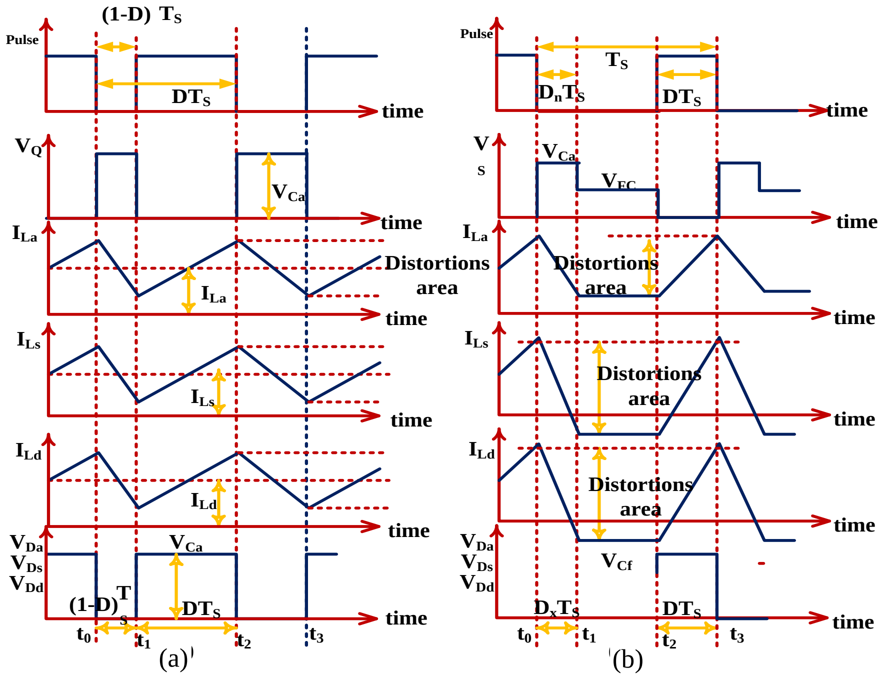

Figure 7. The converter operating modes are (a) CCM, plus (b) DCM [20]

3.2. Working of the converter at the mode-II & III stages

When the MOSFET turns OFF, the energy stored in the inductor and capacitors is transferred to the output. All diodes become forward-biased, forming a series connection of C_x, C_d, C_e. The capacitor and inductor dynamics during this interval are governed by:

$$\begin{cases} I_{Ce-ding} = I_{Cq-ding} + I_{Ld} + I_{Ld-cing} - I_{Ls} \\ I_{Cz-cing} = -I_{Ce-ding} + I_{La} - I_{Ls} + I_{Cd-cing} \\ I_{Cg-cing} = I_{Cz-ding} + I_{Ld} - I_{Rg} \end{cases} \quad (15)$$

$$\begin{cases} V_{Lz} = V_F \\ V_{Le} = -V_{Ce} = -V_{Cd} \\ V_{Ld} = V_{Cz} + V_{Cd} - V_{Cf} - V_{Ce} \end{cases} \quad (16)$$

$$I_{Lz-min} + I_{Le-min} + I_{Ld-min} = 0 \quad (17)$$

$$V_{Lx} = V_{Ly} = V_{Lz} = 0 \quad (18)$$

This stage is responsible for the voltage multiplication effect. Since the capacitors become effectively connected in series, the output voltage rises significantly above the input level.

3.3. Analysis of SSHVCR DC-DC converter under steady state

From the waveforms in Figure 6 and the capacitor charge balance, the filter capacitor voltages in steady state can be expressed as (19).

$$\text{Gain}_{\text{CCM}} = \frac{V_g}{V_{FC}} = \frac{1+2D}{1-D} \tag{19}$$

The second charge concept is utilized for the capacitor captured, plus the delivered currents are obtained as (20).

$$\begin{cases} I_{Cg-cing} = I_g * \frac{D}{1-D} = \frac{\text{Gain}_{\text{CCM}}-1}{3} * I_g \\ I_{Cg-ding} = I_g \end{cases} \tag{20}$$

The root mean square (RMS) value of all the switches, plus passive components, is derived as (21)-(24).

$$I_{Q_{RMS}} = \sqrt{(\text{Gain}_{\text{CCM}} + 2)(\text{Gain}_{\text{CCM}} - 1)} * I_g \tag{21}$$

$$I_{Da-_{RMS}} = I_{Ds-_{RMS}} = I_{Dd-_{RMS}} = \sqrt{\frac{\text{Gain}_{\text{CCM}}+2}{3}} * I_g \tag{22}$$

$$I_{Cs-_{RMS}} = I_{Ca-_{RMS}} = \sqrt[2]{\frac{\text{Gain}_{\text{CCM}}-1}{3}} * I_g \tag{23}$$

$$I_{Cd-_{RMS}} = I_{Cf-_{RMS}} = I_{Cg-_{RMS}} = \sqrt{\frac{\text{Gain}_{\text{CCM}}-1}{3}} * I_g \tag{24}$$

3.4. Mode-III operation (transition or DCM state)

If the inductor current reaches zero before the switching cycle ends, the converter enters discontinuous conduction mode (DCM). In this mode, all semiconductor devices are OFF, and the load is supplied only by capacitor discharge. The corresponding capacitor and inductor expressions are (25).

$$\text{Gain}_{\text{DCM}} = \frac{1}{2}\left(1 + \sqrt{1 + \frac{2D^2}{\eta}}\right) \tag{25}$$

Table 1 compares different high-gain DC–DC converter topologies in terms of voltage gain, component count, grounding requirement, energy storage elements, output current nature, and device voltage stress [21]. The comparison highlights the trade-off between circuit complexity, achievable gain, and voltage stress. The proposed SSHVCR-BC demonstrates high voltage gain with uniform output current and reduced device stress, making it suitable for fuel-cell applications [22].

Table 1. Comparative assessment of the proposed converter circuit with existing topologies [21]

Converter type	Voltage gain expression	Power devices used	Ground requirement	Energy storage components	Output current nature	Switch voltage stress	Diode voltage stress
QTSCN [21]	(1 + 3D)/ (1 - D)	One switch and three diodes	Yes	Two inductors and capacitors	Uniform	1	1
SWOBC [23]	(3-D)/ (1 - D)	One switch and four diodes	No	Single inductor and four capacitors	Distorted	$\frac{\text{Gain}_{\text{CCM}} - 1}{2 * \text{Gain}_{\text{CCM}}}$	$\frac{\text{Gain}_{\text{CCM}} - 1}{2 * \text{Gain}_{\text{CCM}}}$
HITBLC [4]	2/ (1 - D)	Three switches and two diodes	Yes	Two inductors and capacitors	Distorted	0.5	0.5
GBBC [24]	1/ (1 - D)	One switch and one diode	No	One inductor and one capacitor	Uniform	1	1
SSHVCR BC	(1 + 2D)/ (1 - D)	One switch and three diodes	Yes	Three inductors and five capacitors	Uniform	$\frac{\text{Gain}_{\text{CCM}} + 2}{3 * \text{Gain}_{\text{CCM}}}$	$\frac{\text{Gain}_{\text{CCM}} + 2}{3 * \text{Gain}_{\text{CCM}}}$
SSZVBC [25]	(2 + D)/ (1 - D)	Two switches and three diodes	No	Three inductors and three capacitors	Distorted	0.5	0.5
SSLVBC [25]	(1 + D)/ (1 - D)	One switch and three diodes	No	Two inductors and three capacitors	Uniform	$\frac{1 + \text{Gain}_{\text{CCM}}}{2 * \text{Gain}_{\text{CCM}}}$	$\frac{1 + \text{Gain}_{\text{CCM}}}{2 * \text{Gain}_{\text{CCM}}}$

4. RESULTS AND DISCUSSION

The performance of the proposed SSHVCR converter with fuzzy MPPT was evaluated in MATLAB/Simulink using a PEM fuel-cell input (30–60 V). Figures 8 to 10 summarize the key results. Figure 8(a) shows the V–I characteristics of the PEMFC, where the output voltage decreases at higher current densities due to activation, ohmic, and concentration losses. This justifies the necessity of a high-gain converter to boost the low stack voltage. Figure 8(b) shows that convergence and oscillations are low, and the fuzzy MPPT the duty-cycle converges to approximately 60% within 1.5 seconds and therefore controls the duty-cycle smoothly and rapidly.

The voltage boosting capability is validated in Figure 8(c), where the converter raises the input range of 30–60 V to above 200 V, confirming the high-gain nature of the SSHVCR. Figure 8(d) illustrates the output ripple, which was kept within a range of about 1 Vpp, which proves the efficiency of the capacitor-based filtering network and the charge-discharge homogeneity. The methods of MPPT are compared in Figure 9. P&O oscillates around MPP, and IC minimizes oscillation, although slower responsive to dynamic changes. The suggested fuzzy MPPT provides the quickest convergence as it converges to more than 99% of optimal power in a short period of time with a small overshoot. This demonstration shows that FLC is suitable for non-linear switched-capacitor converters.

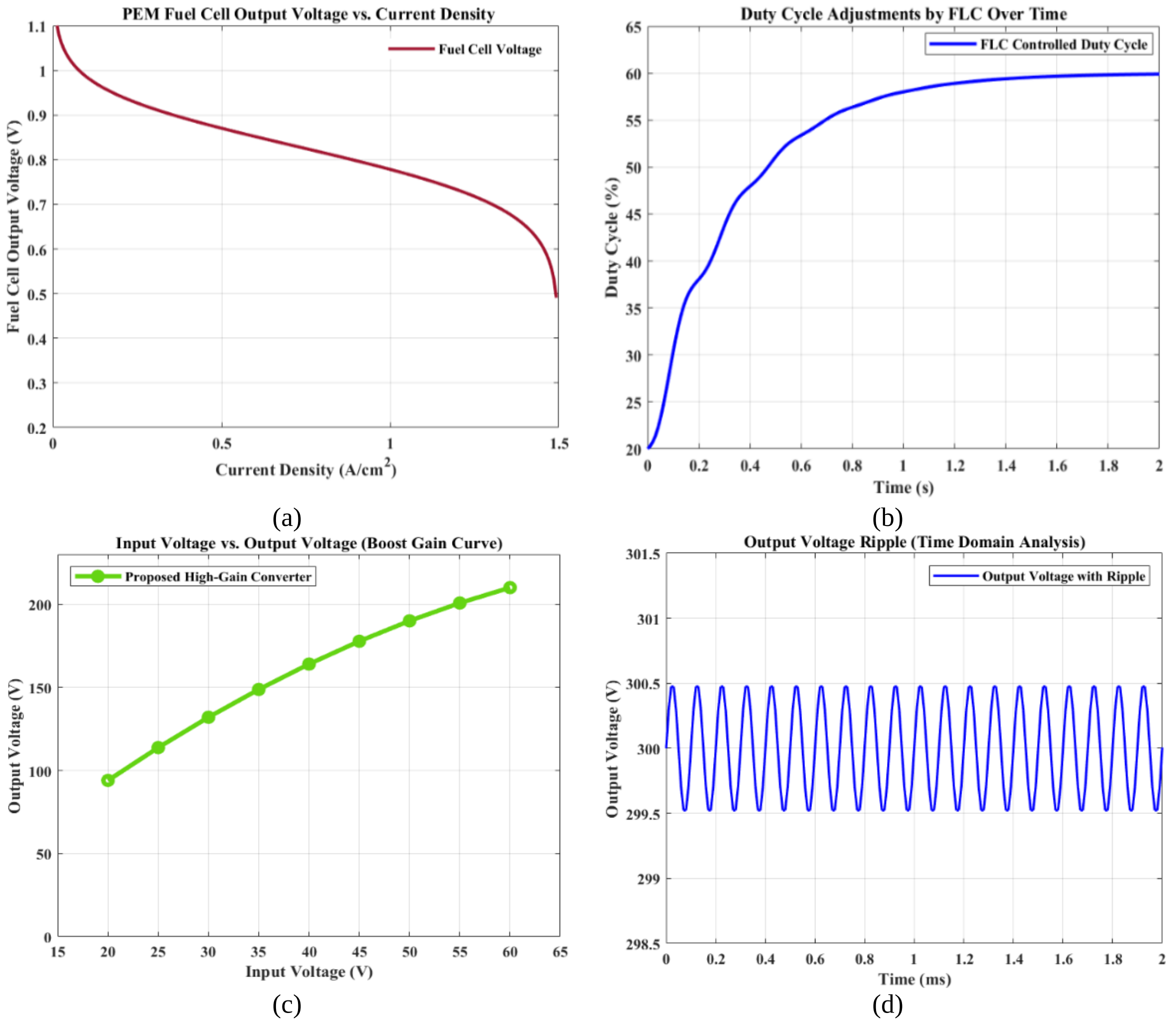

Figure 8. Performance characteristics of the PEM fuel cell–based high-gain converter system: (a) fuel cell output voltage versus current density, (b) duty-cycle adjustment using FLC, (c) input–output voltage characteristics, and (d) output voltage ripple [23]

Figure 10(a) indicates that the converter is most efficient at medium load (200-250 W), approximately 94-95%. In the case of step load disturbance (Figure 10(b)), the voltage across the output rapidly converts to 300 V, which depicts a robust performance of a transient nature. The fuzzy inference surface in Figure 10(c) shows the error variable versus the change in error variable in a smooth manner, allowing duty-cycle adjustment to be stable. The radar comparison in Figure 10(d) indicates that SSHVCR is a high-voltage converter with greater voltage gain and quality of output and efficiency, and less device stress, demonstrating that the device is suitable for high-voltage automotive applications. In general, it can be concluded that, according to the simulation results, the proposed converter system, together with the fuzzy MPPT, satisfies high-gain, low-ripple, and stable dynamic response parameters of electric vehicle powertrains based on fuel cells.

(a)

(b)

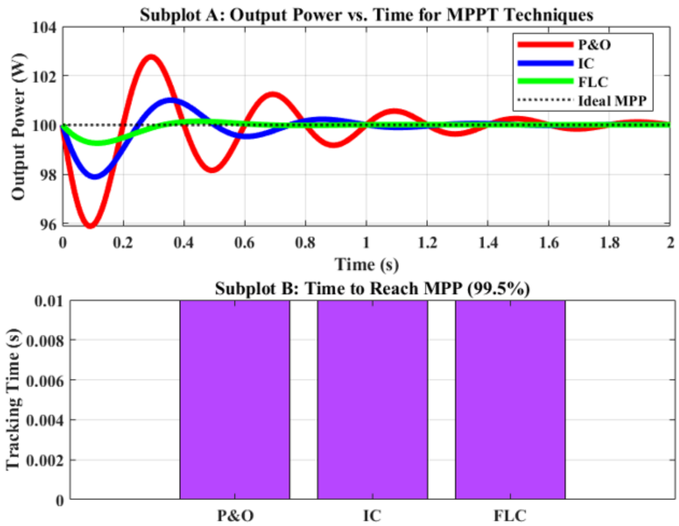

Figure 9. The methods: (a) output power vs time for MPPT techniques and (b) tracking time to reach MPP [24]

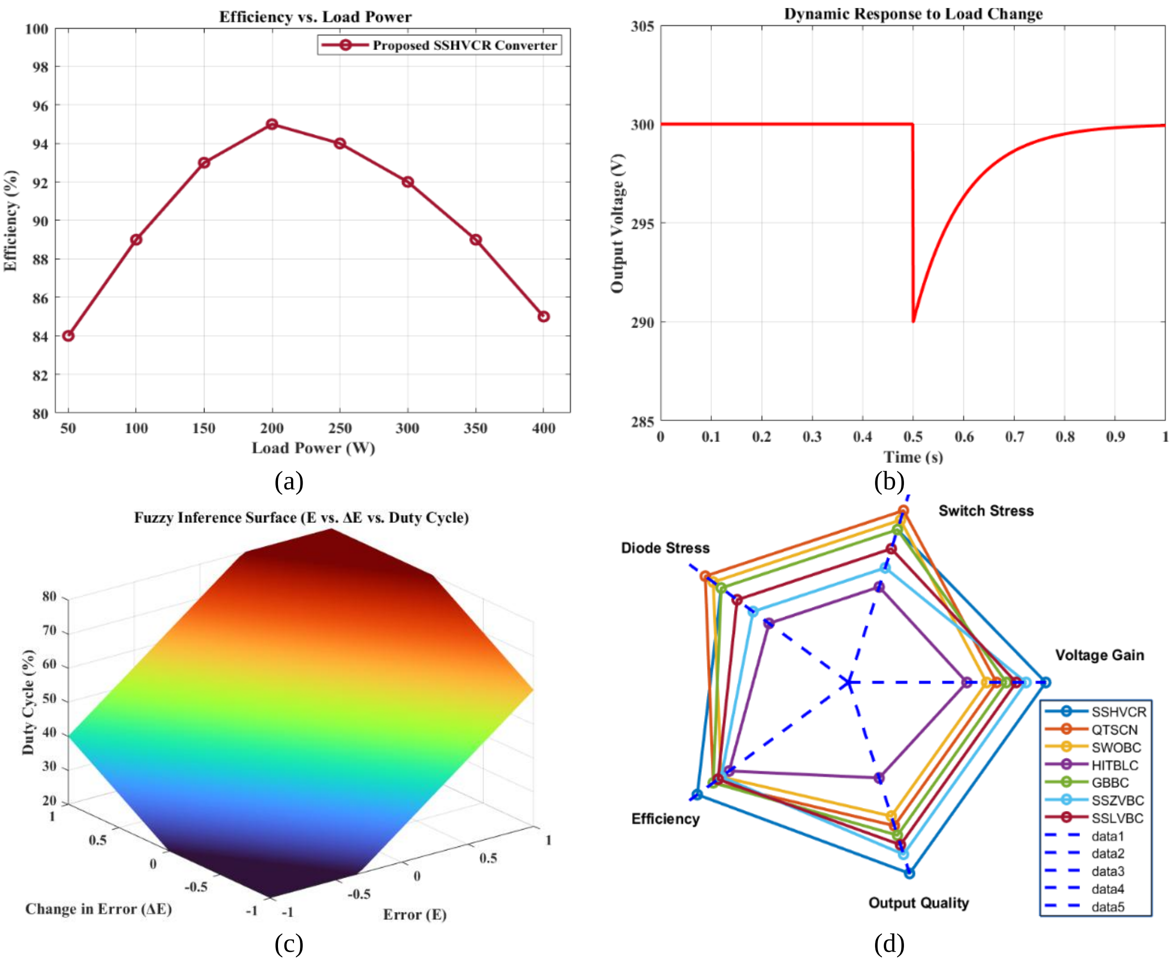

Figure 10. Dynamic and performance characteristics of the proposed converter: (a) efficiency versus load power, (b) dynamic response to load change, (c) fuzzy inference surface, and (d) radar plot comparing converters

5. CONCLUSION

In this paper, a high-gain switched-capacitor DC-DC converter (SSHVCR) is proposed and integrated with a fuzzy logic-based MPPT controller in the applications of a hydrogen fuel cell vehicle. The topology proposed provides greater than 300 V output voltage when it uses a 30-60 V fuel cell PEM input, yet uses no large magnetic devices. The simulation findings are low ripple (<1 Vpp) at the output, quick MPPT settling (1.5 s to 99.5% of MPP), and the peak efficiency is approximately 94.5% 94.5%. The converter also exhibits a good transient response to changes in the load. Compared to the existing converter topologies, SSHVCR is observed to offer better voltage gain and balanced device stress. The combination of fuzzy MPPT also improves stability and power recovery thus the proposed system represents a promising solution for next generation hydrogen powered electric vehicles.

FUNDING INFORMATION

The research work was carried out without any external financial support.

AUTHOR CONTRIBUTIONS STATEMENT

This journal uses Contributor Roles Taxonomy (CRediT) to recognize individual author contributions, reduce authorship disputes, and facilitate collaboration.

Name of Author	C	M	So	Va	Fo	I	R	D	O	E	Vi	Su	P	Fu
Gaddala Anusha	✓	✓	✓	✓	✓	✓		✓	✓	✓	✓		✓	✓
A. V. V. Sudhakar		✓	✓			✓			✓	✓	✓	✓	✓	
Shaik Rafikiran	✓		✓	✓			✓		✓		✓	✓	✓	
Ram Ragotham Deshmukh	✓			✓					✓			✓		
C. H. Hussaian Basha		✓							✓	✓				✓

C : **C**onceptualization
M : **M**ethodology
So : **So**ftware
Va : **Va**lidation
Fo : **Fo**rmal analysis
I : **I**nvestigation
R : **R**esources
D : **D**ata Curation
O : Writing - **O**riginal Draft
E : Writing - Review & **E**diting
Vi : **Vi**sualization
Su : **Su**pervision
P : **P**roject administration
Fu : **Fu**nding acquisition

CONFLICT OF INTEREST STATEMENT

The authors declare that they have no known competing financial interests or personal relationships that could have appeared to influence the work reported in this paper.

DATA AVAILABILITY

Data availability is not applicable to this paper as no new data were created or analyzed in this study.

REFERENCES

[1] B. Eswaraiah and K. Balakrishna, "A novel on high voltage conversion ratio DC-DC converter for EV-fed fuel cell application with hybrid MPPT controller," *International Journal of Circuit Theory and Applications*, vol. 52, no. 4, pp. 1962–1993, 2024, doi: 10.1002/cta.3851.

[2] N. Swaminathan and N. Lakshminarasamma, "The steady-state DC gain loss model, efficiency model, and the design guidelines for high-power, high-gain, low-input voltage DC-DC converter," *IEEE Transactions on Industry Applications*, vol. 54, no. 2, pp. 1542–1554, 2018, doi: 10.1109/TIA.2017.2779099.

[3] A. Beşkardeş, Y. Hameş, and K. Kaya, "A comprehensive review on fuzzy logic control systems for all, hybrid, and fuel cell electric vehicles," *Soft Computing*, vol. 28, no. 13–14, pp. 8183–8221, 2024, doi: 10.1007/s00500-023-09454-5.

[4] M. Singh, M. R. Yadav, and D. K. Dhaked, "A review on various voltage boosting topology in DC-DC converter," *Recent Advances in Electrical & Electronic Engineering (Formerly Recent Patents on Electrical & Electronic Engineering)*, vol. 17, no. 6, pp. 554–572, 2024.

[5] M. Süleyman and T. V. Mumcu, "Neuro-fuzzy scheme plus optimal PI control for controlling DC–DC converters," *Science Progress*, vol. 108, no. 1, 2025, doi: 10.1177/00368504241288790.

[6] Z. A. Ghani *et al.*, "Development of a DC to DC buck converter for photovoltaic application utilizing peripheral interface controller," *ARPN Journal of Engineering and Applied Sciences*, vol. 14, no. 7, pp. 1317–1324, 2019.

[7] F. Cai, S. Cai, and Z. Tu, "Proton exchange membrane fuel cell (PEMFC) operation in high current density (HCD): Problem, progress and perspective," *Energy Conversion and Management*, vol. 307, 2024, doi: 10.1016/j.enconman.2024.118348.

[8] C. Lamy, "From hydrogen production by water electrolysis to its utilization in a PEM fuel cell or in a SO fuel cell: Some considerations on the energy efficiencies," *International Journal of Hydrogen Energy*, vol. 41, no. 34, pp. 15415–15425, 2016, doi: 10.1016/j.ijhydene.2016.04.173.
[9] D. Feng, C. Bao, and T. Gao, "Prediction of overpotential and concentration profiles in solid oxide fuel cell based on improved analytical model of charge and mass transfer," *Journal of Power Sources*, vol. 449, , 2020, doi: 10.1016/j.jpowsour.2019.227499.
[10] I. S. Martín, A. Ursúa, and P. Sanchis, "Modelling of PEM fuel cell performance: Steady-state and dynamic experimental validation," *Energies*, vol. 7, no. 2, pp. 670–700, 2014.
[11] A. Kumar, P. Chaudhary, and M. Rizwan, "Development of fuzzy logic based MPPT controller for PV system at varying meteorological parameters," in *2015 Annual IEEE India Conference (INDICON)*, Dec. 2015, pp. 1–6. doi: 10.1109/INDICON.2015.7443203.
[12] B. E. Elnagi, A. M. Ismaiel, H. S. E. Mansour, and M. N. Abd-Alwahab, "Fuel cell stack design and modelling with a double-stage boost converter coupled to a single-phase inverter," *Clean Energy*, vol. 8, no. 1, pp. 188–196, 2024, doi: 10.1093/ce/zkad083.
[13] H. H. H. Mousa, A. R. Youssef, I. Hamdan, M. Ahamed, and E. E. M. Mohamed, "Performance assessment of robust PO algorithm using optimal hypothetical position of generator speed," *IEEE Access*, vol. 9, pp. 30469–30485, 2021, doi: 10.1109/ACCESS.2021.3059884.
[14] A. Chellakhi, S. El Beid, and Y. Abouelmahjoub, "An innovative fast-converging speed MPPT approach without oscillation for temperature varying in photovoltaic systems applications," *Energy Sources, Part A: Recovery, Utilization and Environmental Effects*, vol. 44, no. 2, pp. 2674–2696, 2022, doi: 10.1080/15567036.2022.2058121.
[15] C. Sun, J. Ling, and J. Wang, "Research on a novel and improved incremental conductance method," *Scientific Reports*, vol. 12, no. 1, p. 15700, 2022, doi: 10.1038/s41598-022-20133-7.
[16] S. R. Zahra and M. A. Chishti, "Fuzzy logic and fog based secure architecture for internet of things (FLFSIoT)," *Journal of Ambient Intelligence and Humanized Computing*, vol. 14, no. 5, pp. 5903–5927, 2023, doi: 10.1007/s12652-020-02128-2.
[17] M. K. Kazimierczuk, D. K. Saini, and A. Ayachit, *Average current-mode control of DC-DC power converters*. John Wiley & Sons. 2022. doi: 10.1002/9781119525592.
[18] H. Bi, P. Wang, and Y. Che, "A capacitor clamped H-Type Boost DC-DC converter with wide voltage-gain range for fuel cell vehicles," *IEEE Transactions on Vehicular Technology*, vol. 68, no. 1, pp. 276–290, 2019, doi: 10.1109/TVT.2018.2884890.
[19] Z. A. Ghani *et al.*, "Peripheral interface controller-based maximum power point tracking algorithm for photovoltaic dc to dc boost controller," *Telkomnika (Telecommunication Computing Electronics and Control)*, vol. 18, no. 1, pp. 240–250, 2020, doi: 10.12928/telkomnika.v18i1.12730.
[20] F. Gutierrez, "Fully-integrated converter for low-cost and low-size power supply in internet-of-things applications," *Electronics (Switzerland)*, vol. 6, no. 2, p. 38, 2017, doi: 10.3390/electronics6020038.
[21] M. Zhou, J. Fu, X. Wu, M. Yang, and Z. Zhang, "A Non-isolated High-gain DC/DC converter suitable for fuel cell vehicles," *Journal of Electrical Engineering and Technology*, vol. 17, no. 1, pp. 271–282, 2022, doi: 10.1007/s42835-021-00785-7.
[22] S. Kovvali, N. Jayaram, S. V. K. Pulavarthi, Y. R. Shankar, J. Rajesh, and V. G. Prasant, "Quadruple boost switched capacitor-based inverter for standalone applications," *IEEE Access*, vol. 11, pp. 30442–30458, 2023, doi: 10.1109/ACCESS.2023.3260257.
[23] M. A. B. Kumar and V. Krishnasamy, "A single-switch continuous input current buck-boost converter with noninverted output voltage," *IEEE Transactions on Power Electronics*, vol. 38, no. 2, pp. 2181–2190, 2023, doi: 10.1109/TPEL.2022.3215179.
[24] Y. Ye, M. Chen, X. Wang, and L. Cao, "Boost-type common-ground PV inverter based on quasi-Z-source and switched-capacitor," *International Journal of Electrical Power and Energy Systems*, vol. 144, p. 108522, 2023, doi: 10.1016/j.ijepes.2022.108522.
[25] B. E. Elnaghi, M. E. Dessouki, M. N. Abd-Alwahab, and E. E. Elkholy, "Development and implementation of two-stage boost converter for single-phase inverter without transformer for PV systems," *International Journal of Electrical and Computer Engineering*, vol. 10, no. 1, pp. 660–669, 2020, doi: 10.11591/ijece.v10i1.pp660-669.

BIOGRAPHIES OF AUTHORS

Gaddala Anusha is a research scholar in the Department of Electrical and Electronics Engineering at S. R. University, Warangal. She is pursuing her Ph.D. in power electronics with a focus on high-gain DC–DC converters and intelligent MPPT techniques for hydrogen and electric vehicle applications. She holds an M.Tech. in power electronics and a B.Tech. in electrical and electronics engineering. Her research interests include fuel cell systems, renewable energy integration, and MATLAB/Simulink-based converter modelling. She can be contacted at email: 2305c20004@sru.edu.in.

Dr. A. V. V. Sudhakar is a professor in the Department of Electrical and Electronics Engineering at S. R. University, Warangal. He holds a Ph.D. in power systems from JNTU Hyderabad and has over 23 years of experience in power system operation, renewable energy integration, smart grids, and EV charging systems. His current work focuses on intelligent algorithms for multi-area power system operation. He can be contacted at email: avv.sudhakar@sru.edu.in.

Dr. Shaik Rafikiran is a professor at S V College of Engineering, India, and an Editorial Board Member of Scientific Reports (Nature Portfolio). His research expertise includes MPPT controllers, solar PV systems, fuel cells, fuzzy logic techniques, and DC–DC converters. He has made significant contributions to renewable energy and power electronics and actively mentors research scholars while collaborating on high-impact international publications. He can be contacted at email: rafikiran@gmail.com.

Dr. Ram Raghotham Deshmukh is a professor in the Department of Electrical and Electronics Engineering at SR University, Warangal. He holds a Ph.D. in Electrical Engineering from Cardiff University, United Kingdom, and brings over 20 years of academic and industry experience, including key engineeri
ng roles in the United Kingdom. His research interests include electrical machines, electric vehicles, and artificial intelligence applications in power systems. He currently serves as the Director of Training and Placements at SR University. He can be contacted at email: ramdeshmukh@sru.edu.in.

Dr. C. H. Hussaian Basha is a senior assistant professor in the Department of Electrical and Electronics Engineering at SR University, Warangal. He holds a Ph.D. from VIT University and an M.Tech. in Power Electronics and Drives. His research focuses on single-switch DC–DC converters, AI-based MPPT controllers, hydrogen-vehicle power converters, and V2G/G2V energy management. He can be contacted at hussaian.basha@sru.edu.in.